Coligand Effects on Bonding Mode. Synthesis and Properties of (Diallylmalonato)platinum(II) Complexes of P vs. N Donating Ligand

Ok-Sang Jung,* Young-A Lee, Sung Ho Park, and Kyung Ho Yoo†

Materials Chemistry Research Center, Korea Institute of Science and Technology, Seoul 136-791, Korea

†Medicinal Chemistry Reseach Center, Korea Institute of Science and Technology, Seoul 136-791, Korea

(Received March 29, 1999)

The reaction of *cis*-[$Pt^{II}(OH)_2A_2$] (A = triethylphosphine (PEt_3); A_2 = tetrahydro-4*H*-pyran-4,4-dimethanamine (hpda)) with diallylmalonic acid in aqueous solution affords *cis*-[Pt(dam)A_2] (dam = diallylmalonate). The bonding mode of the dam is dependent upon the donation effect of the phosphine vs the nitrogen coligand. The crystal structure of *cis*-[Pt(dam)(PEt_3)$_2$] ($C_{21}H_{40}O_4P_2Pt\cdot H_2O$: monoclinic $P2_1/c$, a = 13.918(2), b = 12.464(1), c = 15.737(1) Å, β = 107.097(8)°, V = 2609.4(4) Å^3, Z = 4, R = 0.033) discloses that the dam is bonded to the platinum atom in a (κ^2O_3)-mode (Pt–O = 2.057(4), 2.061(4) Å) with two phosphine ligands in the *cis* position. In contrast, for *cis*-[Pt(dam)(hpda)] ($C_{16}H_{16}N_2O_5Pt\cdot 4.5H_2O$: monoclinic $C2/c$, a = 28.250(3), b = 11.169(1), c = 13.368(4) Å, β = 94.16(1)°, V = 4207(1) Å^3, Z = 8, R = 0.0293), the dam ligand is chelated to the platinum(II) ion in a ($\kappa O,\eta^2$-*C*,*C*)-mode (Pt–O = 2.004(4) Å; Pt–C = 2.089(6), 2.101(6) Å) in the solid state. *cis*-[Pt(κ^2O_3-dam)(PEt_3)$_2$] easily reacts with KBr pellet matrix for IR measurements while *cis*-[Pt($\kappa O,\eta^2$-*C*,*C*-dam)(hpda)] is inert in the pellet. In solution, however, the structure of *cis*-[Pt(κ^2O_3-dam)(PEt_3)$_2$] is locked, whereas *cis*-[Pt($\kappa O,\eta^2$-*C*,*C*-dam)(hpda)] can be isomerized to *cis*-[Pt(κ^2O_3-dam)(hpda)].

The ability to modulate the structural and physical properties by means of chemical triggers is of central importance in the development of molecular materials.[1—4] An increasing effort has been presently directed towards the design of dynamic molecules for use as switching molecules. Investigations on ambidentate ligands as sensitive probes via electronic or steric changes have resulted in numerous publications. The chemical behaviors of ambidentate ligands are subtly dependent upon various factors, such as the acceptor nature of central metals, the electronic and steric effects of ligands and coligands, solvents, pH, and temperature.[5—9] In particular, their labile bonding modes have often been used to deduce general structure-stability relationships, and the results can be extended beyond the initial studies to such diverse areas as quantum mechanical calculations, molecular switches, and isomeric catalysts. Such examples mainly come from chelate ligands bearing one strong and one weak donor atom. In this context, it is worth scrutinizing the class of (diallylmalonato)platinum(II) complexes. First, the central platinum ion is a Lewis acid that can form various different linkage isomers.[10,11] Second, the platinum environment provided by the diallylmalonato ligand might serve as a model for structure-biological activity. Third, delicate tuning of the bonding mode could serve the development of switching materials or solvent recognition.

The exploitation of diallylmalonate (dam) (Chart 1) as a rational strategy has until recently remained unexplored. This article reports on the synthesis, coordination mode, and related properties of (diallylmalonato)platinum(II) complexes of bis(triethylphosphine) vs. tetrahydro-4*H*-pyran-4,4-dimethanamine (hpda). The dam is an ambidentate ligand that consists of four functional groups with appropriate angle and flexibility, and the ligand may chelate to a metal ion in one of the three possible carbxylate–carboxylate, carboxylate–alkene, and alkene–alkene modes.

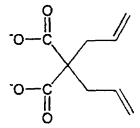

dam

Chart 1.

Experimental

Materials and Instrumentation. Reagent-grade potassium tetrachloroplatinate(II) (Kojima) and triethylphosphine (Aldrich) were used as received. Diethyl diallylmalonate (Aldrich) was converted to its corresponding acid (Hdam) by a standard method.[12] Tetrahydro-4*H*-pyran-4,4-dimethanamine (hpda),[13] *cis*-[Pt(NO_3)$_2$(PEt_3)$_2$],[14] and *cis*-[Pt(NO_3)$_2$(hpda)] [14] were prepared by respective literature method. ^{1}H, ^{13}C, and ^{31}P NMR spectra were recorded on a Varian Gemini 300 instrument operating at 300.00, 75.48, and 121.44 MHz, respectively. The chemical shifts were relative to internal Me_4Si (^{1}H and ^{13}C) and external $(C_6H_5O)_3PO$ (^{31}P) for the indicated nuclei. The infrared spectra in the 5000—400 cm^{-1} region were measured as alkaline metal halide pellets on a Perkin–Elmer 16F PC model FT-IR spectrometer. Elemental analysis was performed at the Advanced Analysis Center at KIST.

***cis*-[Pt(dam)(PEt$_3$)$_2$].** *cis*-[Pt(NO$_3$)$_2$(PEt$_3$)$_2$] (2.22 g, 4.0 mmol) dissolved in water (100 mL) was eluted through an anion-exchange resin (Amberlite IRA-400 (OH)) to obtain a dihydroxo species, *cis*-[Pt(OH)$_2$(PEt$_3$)$_2$], and an additional amount of water (400 mL) was passed through the column. To the dihydroxo solution (pH = 11.0) was added dropwise a solution of Hdam (0.74 g, 4.0 mmol) in water (30 mL). The reaction mixture was stirred for 10 h at room temperature. The resultant solution was condensed to give white solid in quantitative yield. Recrystallization of the crude product from a mixture of ethanol and diethyl ether (1 : 1) afforded colorless crystals of parallelepiped shape suitable for X-ray crystallography. Mp 119—120 °C. Found: C, 39.80; H, 6.68%. Calcd for $C_{21}H_{40}O_4P_2Pt\cdot H_2O$: C, 39.94; H, 6.70%. IR (KBr, cm^{-1}): ν(COO)$_{asym}$, 1646; ν(COO)$_{sym}$, 1352. ^{1}H NMR (CD$_3$OD) δ = 1.19 (dt, CH$_3$, 18H, J (H–H) = 7.6 Hz, J (P–H) = 18.0 Hz), 1.98 (q, CH$_2$P, 12H, J = 7.6 Hz), 2.85 (t, CH$_2$, 4H, J = 6.6 Hz), 5.00—5.12 (m, =CH$_2$, 4H), 5.73—5.87 (m, =CH, 2H). ^{13}C NMR (CD$_3$OD) δ = 8.2, 15.9 (d, $^1J_{P-C}$ = 36.96 Hz), 42.1, 61.3, 118.2, 136.8, 175.1. ^{31}P NMR (CD$_3$OD) δ = 26.73 ($^1J_{Pt-P}$ = 3589.5 Hz).

***cis*-[Pt(dam)(hpda)].** *cis*-[Pt(NO$_3$)$_2$(hpda)] (1.85 g, 4.0 mmol) dissolved in water (100 mL) was eluted through an anion-exchange resin (Amberlite IRA-400 (OH)) to obtain a dihydroxo species, *cis*-[Pt(OH)$_2$(hpda)], and an additional amount of water (400 mL) was passed through the column. To the dihydroxo solution (pH = 11.0) was added dropwise a solution of Hdam (0.74 g, 4.0 mmol) in water (30 mL). The reaction mixture was stirred for 10 h. The reaction solution was evaporated to dryness to obtain a white solid. The crude product was recrystallized from a mixture of water/acetone (1 : 1) to obtain colorless crystals (75% yield). Mp 177 °C (decomp). IR (KBr, cm^{-1}): ν(COO)$_{asym}$, 1650, 1570; ν(COO)$_{sym}$, 1366, 1320. ^{1}H NMR (D$_2$O) δ = 1.31—1.47 (m, CH$_2$ of hpda, 4H), 1.54 (dd, CH$_2$ of dam, 1H, J = 13.5/7.1 Hz), 2.18—2.51 (m, CH$_2$N and CH$_2$ of dam, 7H), 2.68 (d, CH$_2$N, 1H, J = 13.2 Hz), 2.79 (d, CH$_2$N, 1H, J = 13.2 Hz), 3.50—3.62 (m, CH$_2$O, 4H), 4.11 (d, =CH$_2$, 1H, J = 14.9 Hz), 4.53 (d, =CH$_2$, 1H, J = 7.6 Hz), 4.95 (s, =CH$_2$, 1H), 5.00 (d, =CH$_2$, 1H, J = 10.1 Hz), 5.47 (q, =CH, 1H), 5.70 (q, =CH, 1H). ^{13}C NMR (D$_2$O) δ = 29.8, 32.1, 34.3, 35.0, 41.5, 48.3, 49.4, 62.7, 62.8, 64.9, 77.8 (coordinated C=C), 95.9 (coordinated C=C), 118.8 (uncoordinated C=C), 134.7 (uncoordinated C=C), 177.5 (coordinated COO), 180.8 (uncoordinated COO).

X-Ray Analysis of *cis*-[Pt(dam)(PEt$_3$)$_2$] and *cis*-[Pt(dam)-(hpda)]. The X-ray data were collected on an Enraf–Nonius CAD4 automatic diffractometer with graphite-monochromated Mo $K\alpha$ (λ = 0.71073 Å) at ambient temperature (20(2) °C). The unit cell dimensions were based on 25 well-centered reflections by using a least-squares procedure. During the data collection, three standard reflections monitored every hour did not show any significant intensity variation. The data were corrected for Lorentz and polarization effects, and empirically for absorption (azimuthal Ψ-scans of six reflections). The structures were solved by the Patterson method (SHELXS-86), and were refined by full-matrix least squares techniques (SHELXL-93). [15] All non-hydrogen atoms were refined anisotropically. The hydrogen atoms were placed at the calculated positions. Crystal parameters and procedural information corresponding to data collection and a structure refinement are given in Table 1.

Further details concerning the crystal structure investigation for *cis*-[Pt(dam)(PEt$_3$)$_2$] (CCDC No. 127414) and *cis*-[Pt(dam)(hpda)] (CCDC No. 127415) are available on request from the Director of the Cambridge Crystallographic Data Centre, 12 Union Road, GB-Cambridge CB21EZ, (U.K.). The complete F_o–F_c data have been deposited as Document No. 72032 at the Office of the Editor of Bull. Chem. Soc. Jpn.

Results

Synthesis. The reaction of *cis*-[Pt^{II}(OH)$_2$A$_2$] with Hdam

Table 1. Crystallographic Data for *cis*-[Pt(dam)(PEt$_3$)$_2$] and *cis*-[Pt(dam)(hpda)]

Formula	$C_{21}H_{40}O_4P_2Pt\cdot H_2O$	$C_{16}H_{26}O_4N_2Pt\cdot 4.5H_2O$
Fomular weight	631.60	602.55
Space group	$P2_1/c$ (No. 14)	$C2/c$ (No. 15)
a/Å	13.918(2)	28.250(3)
b/Å	12.464(1)	11.169(1)
c/Å	15.737(1)	13.368(3)
β/deg	107.097(8)	94.16(1)
V/Å^3	2609.4(4)	4207(1)
Z	4	8
d/Mg m^3	1.608	1.903
Aabsorption coeff. / mm^{-1}	5.526	6.722
F(000)	1264	2320
Crystal size / mm	0.40 × 0.35 × 0.20	0.42 × 0.40 × 0.40
θ / deg	25	25
Index ranges	$h,k,\pm l$	$h,k,\pm l$
Reflections collected	3844	3375
Independent reflections	3715	3309
Parameters refined	261	258
Goodness of fit	1.099	1.136
R indices [$I > 2\sigma(I)$]	R_1 = 0.0325	R_1 = 0.0239
	wR_2 = 0.0770	wR_2 = 0.0776
R indices (all data)	R_1 = 0.0343	R_1 = 0.0298
	wR_2 = 0.0778	wR_2 = 0.0780
Largest diff. peak and hole / eÅ^{-3}	1.170, −1.293	0.0784, −1.722

$R_1 = \sum||F_o| - |F_c||/\sum|F_o|$. $wR_2 = \{\sum(F_o^2 - F_c^2)^2/\sum wF^4\}^{1/2}$.

in aqueous solution at room temperature afforded the formula of *cis*-[Pt(dam)A_2]. The dam ligand in *cis*-[Pt(dam)$(PEt_3)_2$] is bonded to the platinum atom in an ($\varkappa^2O_3$)-mode with two phosphine coligands in *cis* position whereas the dam in *cis*-[Pt(dam)(hpda)] is chelated to the platinum(II) ion in an ($\varkappa O,\eta^2$-*C,C*)-mode in the solid state (Eq. 1), which will be discussed in detail. The *cis*-[Pt(dam)$(PEt_3)_2$] is a colorless crystalline solid with a sharp melting point, while the amine analogue, *cis*-[Pt(dam)(hpda)], decomposes prior to melting. The two complexes are soluble in common organic solvents. *cis*-[Pt(dam)(hpda)] is soluble in water, and *cis*-[Pt(dam)-$(PEt_3)_2$] is slightly soluble in water. Although the reaction of *cis*-[$PtSO_4$(hpda)] with barium salt of dam smoothly afforded the *cis*-[Pt(dam)(hpda)], the same procedure is not suitable for *cis*-[Pt(dam)$(PEt_3)_2$] presumably owing to low solubility in water.

Crystal Structures of *cis*-[Pt(dam)$(PEt_3)_2$] and *cis*-[Pt-(dam)(hpda)]. The molecular structure of *cis*-[Pt(dam)-$(PEt_3)_2$] is depicted in Fig. 1, and selected bond distances and angles are listed in Table 2.

The local geometry around the platinum(II) atom approximates to a typical square planar arrangement with two phosphorus atoms in *cis* position. The anionic dam ligand is bonded to the platinum(II) atom in ($\varkappa^2O_3$)-mode. The bond lengths of Pt–O (2.057(4); 2.061(4) Å) are significantly longer than the corresponding bonds (2.011(9); 2.03(1) Å) of (DACH)Pt(FM) (DACH = diamincyclohexane; FM = fluorenylidenemalonate) that contains diamine as a coligand.[16] Such a result discloses that the Pt–O bond is strongly dependent on coligand: P donating coligand weakens the Pt–O bond strength relative to N donating coligand. The bond lengths of Pt–P (2.233(2); 2.246(2) Å) are similar to the corresponding bonds of general phosphine–platinum-(II) complexes.[14] The angle of P(1)–Pt–P(2) (96.34(6)°) is splayed out with the concomitant closing of the bite angle of O(1)–Pt–O(3) (85.1(2)°). Thus, the bite angle of the dam ligand is partially responsible for the distortion of square planar platinum geometry. The present crystal consists of discrete molecules in contrast to the hpda analogue

Table 2. Selected Bond Lengths (Å) and Angles (deg) for *cis*-[Pt(dam)$(PEt_3)_2$] and *cis*-[Pt(dam)(hpda)]

cis-[Pt(dam)$(PEt_3)_2$]		*cis*-[Pt(dam)(hpda)]	
Pt–O(1)	2.061(4)	Pt–O(1)	2.005(4)
Pt–O(3)	2.057(4)	Pt–N(1)	2.021(5)
Pt–P(1)	2.246(2)	Pt–N(2)	2.019(4)
Pt–P(2)	2.233(2)	Pt–C(1)	2.089(6)
O(1)–C(1)	1.273(7)	Pt–C(2)	2.101(6)
O(2)–C(1)	1.234(7)	O(1)–C(4)	1.281(7)
O(3)–C(2)	1.279(7)	O(2)–C(4)	1.227(7)
O(4)–C(2)	1.231(7)	O(3)–C(6)	1.245(7)
		O(4)–C(6)	1.233(7)
O(3)–Pt–O(1)	85.1(2)	O(1)–Pt–N(2)	174.7(2)
O(3)–Pt–P(1)	89.9(1)	O(1)–Pt–N(1)	84.8(2)
O(3)–Pt–P(2)	173.2(1)	N(1)–Pt–N(2)	92.8(2)
O(1)–Pt–P(1)	175.0(1)	O(1)–Pt–C(1)	92.6(2)
O(1)–Pt–P(2)	88.6(1)	C(1)–Pt–N(2)	89.0(2)
P(2)–Pt–P(1)	96.34(6)	N(1)–Pt–C(1)	171.2(3)
		O(1)–Pt–C(2)	90.6(2)
		N(2)–Pt–C(2)	93.8(2)
		N(1)–Pt–C(2)	150.4(2)
		C(1)–Pt–C(2)	37.7(3)

that are held together by intermolecular N–H···O hydrogen interactions.[16] The discrete properties seem to be attributed to the better solubility in organic solvents.

The crystal structure of *cis*-[Pt(dam)(hpda)] is shown in Fig. 2, and the relevant bond distances and angles are listed in Table 2. The local geometry around the platinum atom approximates to a square planar arrangement. The most interesting feature is that the anionic dam ligand is chelated to the platinum atom through one carboxylate (Pt–O(1), 2.004(4) Å) and one alkene moiety (Pt–C(1), 2.089(6) Å; Pt–C(2), 2.101(6) Å), resulting in a ($\varkappa O,\eta^2$-*C,C*)-chelation. Thus, another carboxylato and another alkene moiety are dangled. For the coordinated carboxylato ligand, the bond length of C(4)–O(1) (1.281(7) Å) is much longer than that of C(4)–O(2) (1.227(7) Å). The two corresponding bond lengths of the uncoordinated carboxylate are relatively similar (1.245(7); 1.233(7) Å). The coordinated C(1)–C(2) bond length (1.35(1) Å) is longer than the uncoordinated C(8)–C-(9) bond (1.279(9) Å). There exist intermolecular hydrogen

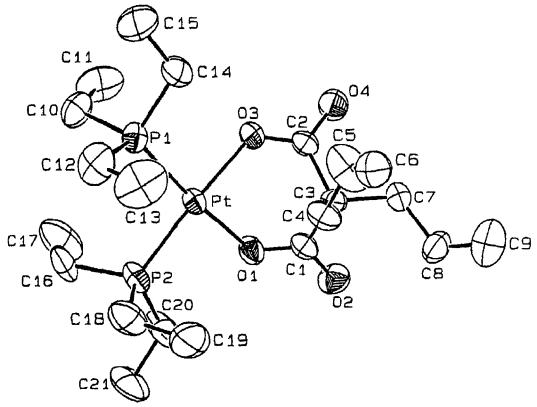

Fig. 1. ORTEP drawing of *cis*-[Pt($\varkappa^2O_3$-dam)$(PEt_3)_2$]·H_2O showing the atomic labeling scheme and thermal ellipsoids at the 50% level. Solvate water molecule and hydrogem atoms are omitted for clarity.

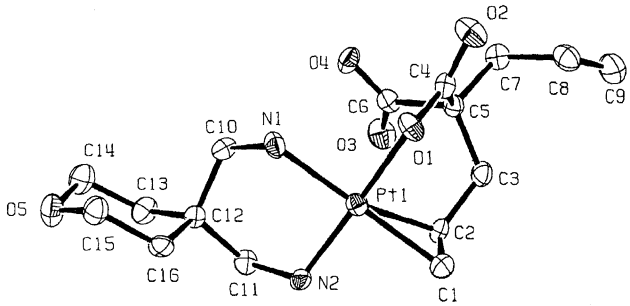

Fig. 2. ORTEP drawing of *cis*-[Pt($\varkappa O,\eta^2$-*C,C*-dam)-(hpda)]·4.5H_2O showing the atomic labeling scheme and thermal ellipsoids at the 50% level. Solvate water molecule and hydrogem atoms are omitted for clarity.

bondings between the oxygen of the coordinated carboxylato group and the amine group of its neighboring molecule (O···N, 2.82—2.97 Å) and between the dangling carboxylato group and the amine group of its neighboring molecule (O···N, 2.91 Å). These intermolecular hydrogen bonds may give rise to additional stability for ($\varkappa O,\eta^2$-*C*,*C*)-chelation in the solid state.

NMR Spectra. The ^{1}H, ^{13}C, and ^{31}P NMR spectra of *cis*-[Pt(dam)(PEt_3)$_2$] were measured in methanol. The NMR spectra suggest that the ($\varkappa^2O_3$)-chelate of the dam unit is retained in solution. In particular, a single carboxylato ^{13}C chemical shift at 175.1 ppm and a single ^{31}P resonance at 26.73 ppm clearly disclose that the ($\varkappa^2O_3$)-chelate of the dam ligand is locked without dissociation or isomerism in solution. A linkage isomerism between alkene and carboxylato group was not observed even in various solvents, such as CD_3OD, Me_2SO-d_6, and D_2O (slightly soluble), in the temperature range of −20—70 °C. Intricate ^{1}H NMR spectrum of *cis*-[Pt(dam)(hpda)] in D_2O was clearly assigned via ^{1}H/^{13}C 2D-heteronuclear spectra shown in Fig. 3. Two carboxylato ^{13}C resonances appear at 180.8 and 177.5 ppm due to the uncoordinated and the coordinated carboxylato group, respectively, in contrast to the corresponding single resonance of *cis*-[Pt(dam)(PEt_3)$_2$] (175.1 ppm in CD_3OD). The two alkene moieties also show two pairs of ^{13}C resonances (77.8, 95.9; 118.8, 134.7 ppm), indicating the coexistence of a coordinated and an uncoordinated alkene moiety, respectively. As expected, the signals of the hpda coligand are fairly complicate due to the unsymmetrical ligation of the dam ligand. Furthermore, the =CH protons of the dam appear as two distinct multiplets (5.47, 5.70 ppm), and the =CH_2 protons lie at four sets of doublets at 4.11; 4.53; 4.95; 5.00 ppm. The *cis*- and *trans*-protons of the =CH_2 protons could be discerned by their coupling constants. Thus, the ($\varkappa O,\eta^2$-*C*,*C*)-mode in *cis*-[Pt(dam)(hpda)] is unambiguously retained in aqueous solution. However, strong solvent effects on the coordination modes were observed, and are designated in Fig. 4. The chemical shifts and peak patterns in CD_3OD are similar to those in D_2O, but the spectrum in CD_3OD shows another set of resonances corresponding to ($\varkappa^2O_3$)-isomer. *cis*-[Pt(dam)(hpda)] exists as an equilibrium of ($\varkappa O,\eta^2$-*C*,*C*) and ($\varkappa^2O_3$)-chelate isomers in methanol. The former species is predominant in a ratio of ($\varkappa O,\eta^2$-*C*,*C*)/($\varkappa^2O_3$) = 4 at room temperature. In contrast, the complex predominantly exists as *cis*-[Pt($\varkappa^2O_3$-dam)(hpda)] in aprotic Me_2SO solution.

IR Spectra. IR spectra of *cis*-[Pt(dam)A_2] have been found to be useful to discern the bonding mode of the carboxylato ligands. The IR spectra of *cis*-[Pt(dam)(PEt_3)$_2$] obtained as KBr pellet are strongly dependent upon time (Fig. 5). The $\Delta\nu$(COO) ($\nu_{asym} - \nu_{sym}$) value (294 cm^{-1})

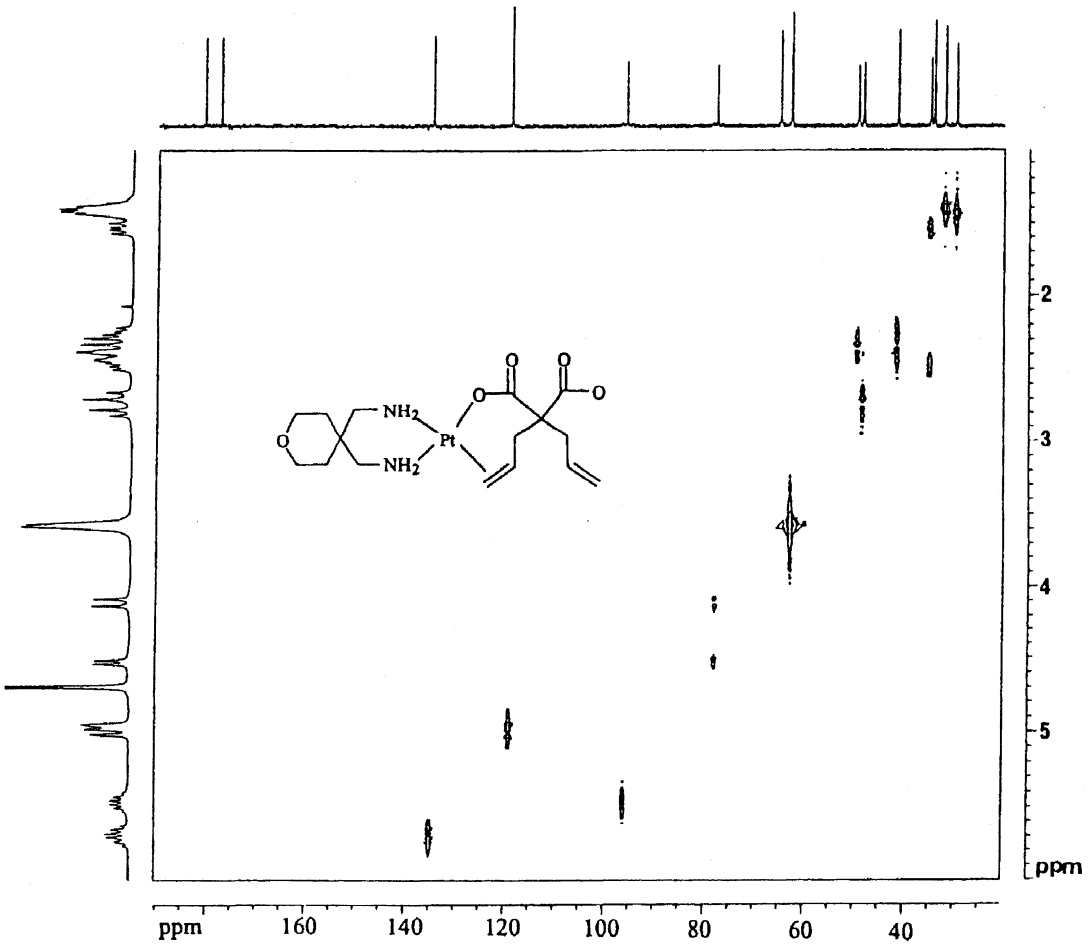

Fig. 3. ^{1}H/^{13}C heteroCOSY NMR spectrum of *cis*-[Pt($\varkappa O,\eta^2$-*C*,*C*-dam)(hpda)]·4.5H_2O in D_2O.

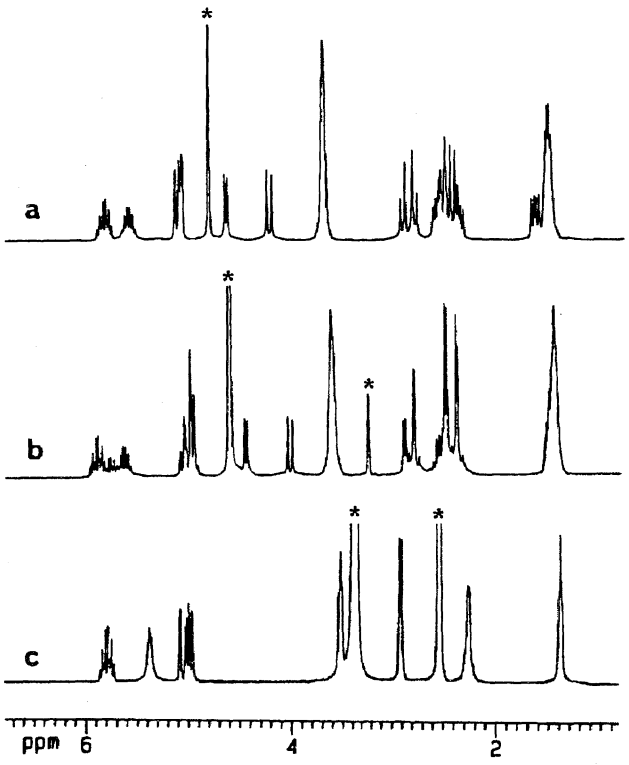

Fig. 4. ^{1}H NMR spectra of *cis*-[Pt($\varkappa O,\eta^2$-*C,C*-dam)-(hpda)·4.5H_2O in D_2O (a), CD_3OD (b), and Me_2SO-d_6 (c), showing ($\varkappa O,\eta^2$-*C,C*)-, ($\varkappa O,\eta^2$-*C,C*)- +($\varkappa^2O_3$)-, and ($\varkappa^2O_3$)-isomer, respectively. Asterisk indicates solvent peak.

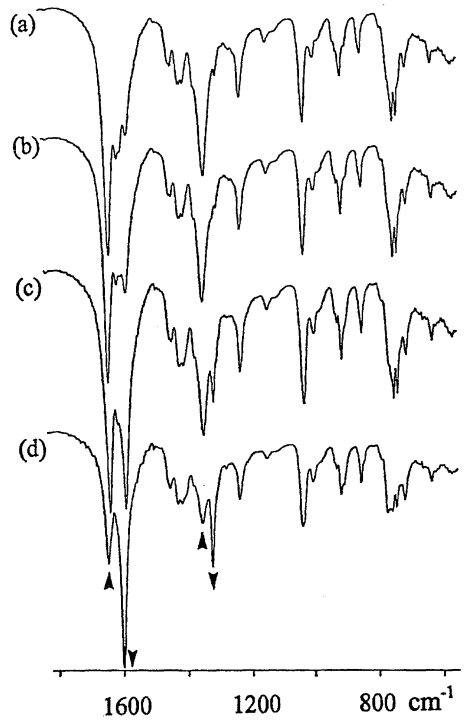

Fig. 5. Time-dependent IR spectra of *cis*-[Pt($\varkappa^2O_3$-dam)-(PEt_3)$_2$]·H_2O measured after 0 min (a); 60 min (b); 100 min (c); 200 min (d) as KBr pellet. New bands (indicated by ↓) corresponds to dissociated carboxylato group of the dam ligand.

larger than 200 cm^{-1} indicates that the carboxylato groups of the dam ligand act as monodentato ligands,[17] consistent with its X-ray crystal structure. A striking feature is that the bands of the carboxylato groups exhibit a marked time-dependence: The band intensity of the asymmetric (1646 cm^{-1}) and symmetric (1352 cm^{-1}) carboxylato stretching frequencies decreases while new bands appear at 1600 and 1324 cm^{-1}. After 4 h, the original bands almost vanish, and the intensities of the new bands prominently increase. The appearance of new bands at the bathochromic shift indicates the formation of a free carboxylato group in the KBr pellet.[17] There are two possibilities, i.e. the ligand can be dissociated from the platinum ion or can be isomerized to Pt-alkene linkage. Furthermore, the complex is promptly reacted with cesium iodide (CsI) that is useful as IR window materials for inorganic compounds. However, for all cases of the changes, the same pattern was observed. Such results suggest that the complex is easily reacted with the alkaline metal halide pellets (Eq. 2). In contrast, for *cis*-[Pt(dam)(hpda)], such a solid reaction hardly occurred at room temperature for more than 1 week. Instead, two pairs of ν(COO) bands ($\nu(COO)_{asym}$, 1650, 1570; $\nu(COO)_{sym}$, 1366, 1320) (Supplementary Material) indicate that the dam is chelated to the metal ion in a ($\varkappa O,\eta^2$-*C,C*)-mode, which is consistent with the chelation mode in water.

Discussion

The steric and electronic requirements of the ligands as well as the acceptor natures of central metals play important roles in their linkage coordinations. For the dam ligand of the present complexes, the alkene moiety is competitive with the carboxylato group in coordination to the platinum(II) ion. Among the three possible bonding modes, the chelation modes of ($\varkappa^2O_3$) and ($\varkappa O,\eta^2$-*C,C*) were observed for *cis*-[Pt-(dam)(PEt_3)$_2$] and *cis*-[Pt(dam)(hpda)], respectively, in the solid state. The difference between the two bonding modes is related to the change in donor strength of PEt_3 and hpda coligands. That is, the prominent difference in the solid state seems to be induced by the electronic effects of the coligands. Of course, such coordination modes may be indebted to the crystal packing energy or intermolecular hydrogen bondings in the solid state.

In solution, the bonding mode of *cis*-[Pt(dam)(PEt_3)$_2$] is inert, whereas the mode of *cis*-[Pt(dam)(hpda)] is labile. In the case of N donating hpda coligand, the bonding barrier of alkene and carboxylato seems to be very similar. The hydrogen bonding ability of solvent with *cis*-[Pt(dam)(hpda)] seems to control the coordination mode of the dam ligand. For instance, the ($\varkappa O,\eta^2$-*C,C*)-chelated species of the complex has zwitterionic form, and thus there seem to be hydrogen bonds between protic solvent molecules and the zwitterionic dipole molecules. Thus, the ($\varkappa O,\eta^2$-*C,C*)-chelate seems to be more stable in protic solvents, whereas the ($\varkappa^2O_3$)-mode is more stable in aprotic solvents, such as Me_2SO or DMF. Methanol is intermediate in polarity, dielectric constant, and hydrogen bonding ability between two extremes, protic H_2O and aprotic Me_2SO. Thus, the

two chelation modes coexist in MeOH at room temperature. Spectral changes observed for the complex in methanol result from an equilibrium between *cis*-[Pt($\varkappa O,\eta^2$-*C,C*-dam)(hpda)] and between *cis*-[Pt($\varkappa^2O_3$-dam)(hpda)] chelate isomers. The solvent-dependent linkage isomerism could be explained by an intramolecular process through a turnstile mechanism (Eq. 3).[18] There is hardly any strain in a square pyramidal coordination, a key intermediate of the isomerism between ($\varkappa^2O_3$)- and ($\varkappa O,\eta^2$-*C,C*)-chelate. For the present system, a solvent is not a simple inert media, but a very important factor along with the central metal and the coligand. For the present system, on all occasions, (alkene,alkene)-chelate was not observed presumably due to the electronic unfavorableness.

In contrast to the behavior of the complexes in solution, *cis*-[Pt(dam)(PEt_3)$_2$] is labile whereas between *cis*-[Pt(dam)-(hpda)] is robust in KBr matrix for IR measurement (Eq. 2). The reaction with KBr pellet seems to be attributed to the ionic character of each complex. For example, the Pt–O bond lengths of *cis*-[Pt(dam)(PEt_3)$_2$] are significantly long compared with diamine analogues,[16] indicating relatively strong ionic character of the Pt–O bond. Thus, the *cis*-[Pt($\varkappa^2O_3$-dam)(PEt_3)$_2$] reacts easily with KBr pellet to form *cis*-[$PtBr_2(PEt_3)_2$] and potassium salt of the free ligand in the solid state. However, *cis*-[Pt($\varkappa O,\eta^2$-*C,C*-dam)(hpda)] is stable in the KBr pellet for more than 1 week.

In conclusion, for (diallylmalonato)platinum(II) complexes, prominent coligand effects on the coordination mode of the dam ligand were observed both in the solid state and in solution. Understanding the features that can be used to control the bonding modes may be a key to the development of complex molecules that exhibit desirable properties.

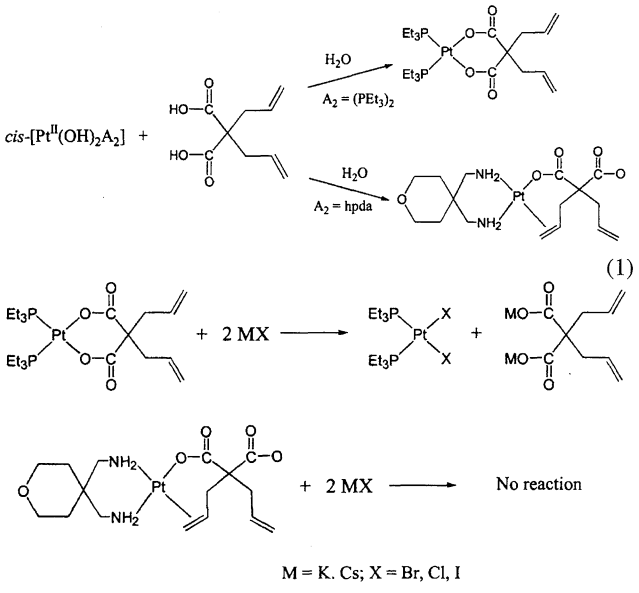

(1)

(2)

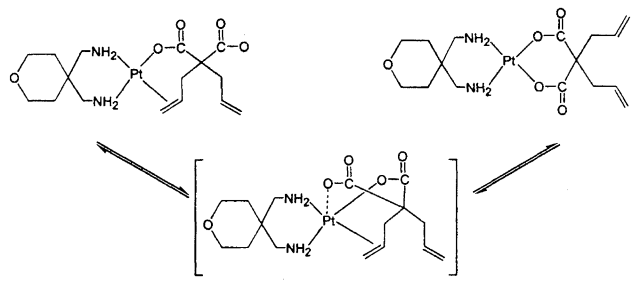

(3)

Support for this research was provided by the Ministry of Science and Technology in Korea.

References

1 A. Gourdon, *New J. Chem.*, **16**, 953 (1988).
2 N. S. Hush, A. T. Wong, G. B. Bacskay, and J. B. Reimers, *J. Am. Chem. Soc.*, **112**, 4192 (1990).
3 O. Kahn, J. Kröber, and C. Jay, *Adv. Mater.*, **4**, 718 (1992).
4 O.-S. Jung, D. H. Jo, Y.-A Lee, and Y. S. Sohn, *Bull. Chem. Soc. Jpn.*, **69**, 2211 (1996).
5 T. G. Appleton, F. J. Pesch, M. Wienken, S. Menzer, and B. Lippert, *Inorg. Chem.*, **31**, 4410 (1992).
6 D. A. Buckingham, *Coord. Chem. Rev.*, **135/136**, 587 (1994).
7 C. A. Bignozzi, C. Chiorboli, M. T. Indelli, F. Scandola, V. Bertolasi, and G. Gilli, *J. Chem. Soc., Dalton Trans.*, **1994**, 2391.
8 D. Das, N. R. Chaudhuri, and A. Ghosh, *Polyhedron*, **15**, 3919 (1996).
9 T. Parac and N. M. Kostic, *J. Am. Chem. Soc.*, **118**, 5946 (1996).
10 P. S. Murdoch, J. D. Ranford, P. J. Sadler, and S. J. Berners-Price, *Inorg. Chem.*, **32**, 2249 (1993).
11 Y. S. Sohn, K. M. Kim, S.-J. Kang, and O.-S. Jung, *Inorg. Chem.*, **35**, 4274 (1996).
12 B. S. Furniss, A. J. Hannaford, P. W. G. Smith, and A. R. Tatchell, "Vogel's Textbook of Practical Organic Chemistry," Longman Scientific & Technical, Great Britain (1989), p. 680.
13 P. Bitha, S. G. Carvajal, R. V. Citarella, R. G. Child, E. F. Delos Santos, T. S. Dunne, F. E. Durr, J. J. Halavaka, S. A. Lang, Jr., H. L. Lindsay, G. O. Morton, T. S. Thomas, R. E. Wallace, Y.-I. Lin, R. Haltiwanger, and C. G. Pierpont, *J. Med. Chem.*, **32**, 2015 (1989).
14 G. Trovo, G. Bandoli, U. Casellato, B. Corain, M. Nicolini, and B. Longato, *Inorg. Chem.*, **29**, 4616 (1990).
15 a) G. M. Sheldrick, "SHELXS-86: A Program for Structure Determination," University of Göttingen, Germany (1986). b) G. M. Sheldrick, "SHELXL-93: A Program for Structure Refinement," University of Göttingen, Germany (1993).
16 Y.-A Lee, O.-S. Jung, S.-J. Kang, and K.-B. Lee, *Inorg. Chem.*, **35**, 1641 (1996).
17 K. Nakamoto, "Infrared and Raman Spectra of Inorganic and Coordination Compounds," 4th ed, John Wiley & Sons, New York (1986), p. 233.
18 J. A. Casares and P. Espinet, *Inorg. Chem.*, **36**, 5428 (1997).